

# Surface Optimization of Glassy Carbon Electrode with Graphitized and Carboxylated Multi-Walled Carbon Nanotubes@ $\beta$ -Cyclodextrin Nanocomposite for Electrochemical Determination of Methyl Parathion

Yu Zhou, Tingting Wu<sup>\*</sup>, Huaibin Zhang, Mengyuan Zhao, Yansheng Shen, Gan Zhu, Meimei Guo, Yunhang Liu, Fang Li, Hongyuan Zhao<sup>\*</sup>

Research Center for Advanced Materials and Electrochemical Technology, School of Mechanical and Electrical Engineering, Henan Institute of Science and Technology, Xinxiang 453003, China

<sup>\*</sup>E-mail: [wtingtingwu@163.com](mailto:wtingtingwu@163.com) (T. Wu), [hongyuanzhao@126.com](mailto:hongyuanzhao@126.com) (H. Zhao)

Received: 2 March 2022 / Accepted: 14 April 2022 / Published: 7 May 2022

---

We reported a simple and low-cost ultrasound-assisted preparation of  $\beta$ -cyclodextrin/graphitized and carboxylated multi-walled carbon nanotubes ( $\beta$ -CD/GR-MWCNTs-COOH) nanocomposite, which was used to modify the glassy carbon electrode (GCE) to fabricate the  $\beta$ -CD/GR-MWCNTs-COOH/GCE sensor for the determination of methyl parathion (MP). The phase structure and surface morphology of  $\beta$ -CD/GR-MWCNTs-COOH nanocomposite was characterized by X-ray diffraction (XRD) and scanning electron microscopy (SEM). For this nanocomposite, GR-MWCNTs-COOH had high electrical conductivity, large specific surface area, and good hydrophilicity;  $\beta$ -CD promoted the uniform dispersion of GR-MWCNTs-COOH and possessed excellent molecular recognition ability for organic molecules. Electrochemical measurements showed that the  $\beta$ -CD/GR-MWCNTs-COOH/GCE sensor presented good MP determination performance with high peak current response due to the synergistic effect of  $\beta$ -CD and GR-MWCNTs-COOH. Under the optimal condition, the fabricated  $\beta$ -CD/GR-MWCNTs-COOH/GCE sensor showed a low limit of detection of 0.027  $\mu$ M in linear MP concentration range of 0.01-15  $\mu$ M. This work has a certain promoting significance for the development of high-performance MP electrochemical sensor.

---

**Keywords:** Electrochemical determination; Methyl parathion; GR-MWCNTs-COOH;  $\beta$ -cyclodextrin; Synergistic effect

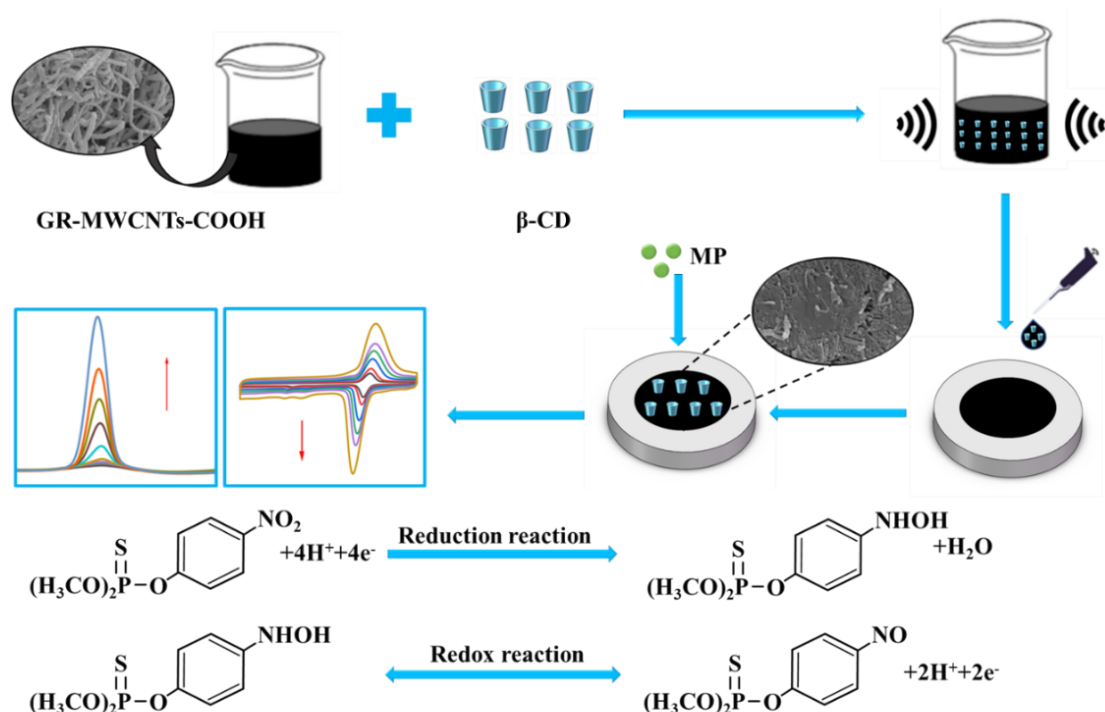
## 1. INTRODUCTION

Organophosphorus pesticides are extremely meaningful for the prevention of diseases and insect pests [1, 2]. As one kind of organophosphorus pesticides, methyl parathion (MP) has been widely used in the field of crop protection [3]. However, the MP residue has a serious impact on human health and

environmental protection [4, 5]. Therefore, it is imperative to develop a rapid, sensitive, and convenient determination method. In recent years, MP detection technology has experienced a rapid development. Electrochemical detection technology has gained more and more interest due to the advantages of simple operation, low cost and high sensitivity [6, 7]. The construction of high-performance electrode provides a new idea for the rapid, accurate and stable detection of MP. According to the reported works [8-11], the determination performance of sensing electrode depends on the modification materials such as carbon materials (carbon nanotubes, graphene, porous carbon), and conductive polymers. Among them, multi-walled carbon nanotubes (MWCNTs) have attracted extensive attention due to their large specific surface area, high electrical conductivity, and hydrophilicity. It has been reported that different types of carbon nanotubes possess different enhancement effects on the electrochemical performance of electrochemical sensors [12, 13]. Compared with the unfunctionalized MWCNTs, the graphitized multi-walled carbon nanotubes (GR-MWCNTs) can help enhance the electric conductivity of carbon nanotubes due to the high graphitization degree and highly ordered graphitic structure [14, 15], and the carboxylated multi-walled carbon nanotubes (MWCNTs-COOH) can present more uniform dispersion effect due to the hydrophilicity of carboxyl functional groups [16, 17]. Ni et al. reported the GR-MWCNTs-based composite modified GCE sensor, which showed excellent electrochemical sensing determination performance [18]. Li et al. fabricated a novel electrochemical sensor based on the MWCNTs-COOH modified GCE, which achieved more sensitive detection of bisphenol A with lower limit of detection compared to the MWCNTs modified GCE sensor [17]. Therefore, the graphitized and carboxylated multi-walled carbon nanotubes (GR-MWCNTs-COOH) was selected as surface modification material to fabricate the electrochemical sensor for the highly sensitive determination of MP.

$\beta$ -cyclodextrin ( $\beta$ -CD) was widely used in fields of biomedicines, food, environmental protection, and agriculture. It has outer edge and hydrophobic inner cavity. The ring structure is composed of hydrophobic inner cavity and water-absorbing outer edge. As a result,  $\beta$ -CD possesses excellent molecular recognition and selection ability for organic molecules [19]. According to the existing literatures [20, 21], the interaction between van der Waals force of  $\beta$ -CD molecule and hydrogen bond of adjacent cyclodextrin can promote the uniform distribution GR-MWCNTs-COOH. Therefore,  $\beta$ -CD can be selected as surface modification material to fabricate the high-performance MP sensor.

In this work, we proposed a simple and low-cost ultrasound-assisted preparation of graphitized and carboxylated multi-walled carbon nanotubes@ $\beta$ -cyclodextrin ( $\beta$ -CD/GR-MWCNTs-COOH) nanocomposite, which was applied to modify the glassy carbon electrode (GCE) for the fabrication of  $\beta$ -CD/GR-MWCNTs-COOH/GCE sensor. The fabrication process and MP determination mechanism of  $\beta$ -CD/GR-MWCNTs-COOH/GCE sensor are shown in **Scheme 1**. GR-MWCNTs-COOH had large specific surface area, high electrical conductivity, and hydrophilicity, and  $\beta$ -CD possessed excellent molecular recognition and selection ability for organic molecules. Combined with their respective advantages, the fabricated  $\beta$ -CD/GR-MWCNTs-COOH/GCE sensor showed excellent electrochemical sensing performance for the determination of MP.



**Scheme 1.** Fabrication of the  $\beta$ -CD/GR-MWCNTs-COOH/GCE sensor for the sensitive determination of MP.

## 2. EXPERIMENTAL

### 2.1 Materials and Reagents

Graphitized and carboxylated multi-walled carbon nanotubes (GR-MWCNTs-COOH),  $\beta$ -cyclodextrin, anhydrous ethanol and dimethylformamide (DMF) were provided by Shanghai Aladdin Biochemical Technology Co., Ltd. Alumina powders with different particle sizes were purchased from CH Instruments Ins.

### 2.2 preparation of $\beta$ -CD/GR-MWCNTs-COOH/GCE Sensor

GR-MWCNTs-COOH (10 mg) was dispersed in 5 mL N, N-dimethylformamide (DMF) under ultrasonic condition to obtain the dispersion solution of GR-MWCNTs-COOH ( $2 \text{ mg mL}^{-1}$ ). Then, a certain amount of  $\beta$ -CD (45 mg) was added to the above suspension with the help of ultrasonic dispersion treatment to obtain the uniform  $\beta$ -CD/GR-MWCNTs-COOH suspension. In order to fabricate the  $\beta$ -CD/GR-MWCNTs-COOH/GCE sensor, the glassy carbon electrode was polished precisely by means of aluminum oxide powder with different particle sizes ( $1.0 \mu\text{m}$ ,  $0.3 \mu\text{m}$  and  $0.05 \mu\text{m}$ ). And then, GCE was rinsed by ethanol and deionized water in ultrasonic cleaner. Subsequently, the  $\beta$ -CD/GR-MWCNTs-COOH/GCE sensor was successfully prepared by dipping the  $\beta$ -CD/GR-MWCNTs-COOH suspension ( $5 \mu\text{L}$ ) on the polished GCE surface followed with infrared drying treatment.

#### 2.4 Characterization and measurement

X-ray diffraction (XRD), Fourier transform infrared spectroscopy (FTIR), and scanning electron microscopy (SEM) were used to investigate the phase structure and surface morphology. The electrochemical behavior of MP at the fabricated sensor were analyzed by cyclic voltammetry (CV) and differential pulse voltammetry (DPV) based on the CHI660E electrochemical workstation. The modified  $\beta$ -CD/GR-MWCNTs-COOH/GCE sensor was used as working electrode, platinum wire as counting electrode and saturated calomel electrode (SCE) as reference electrode.

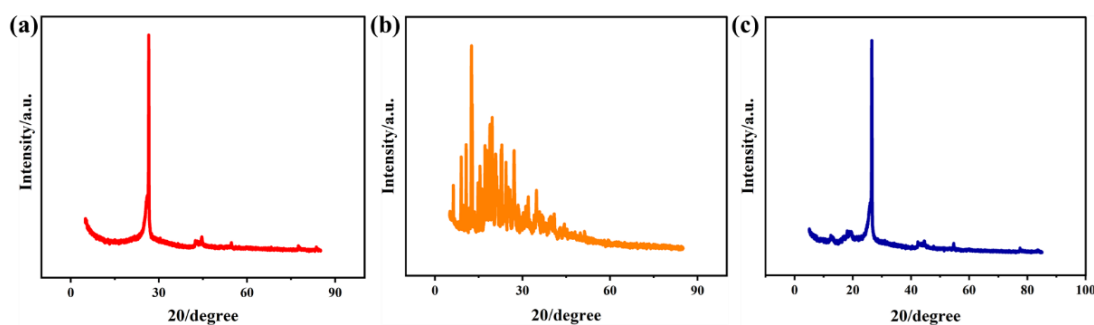
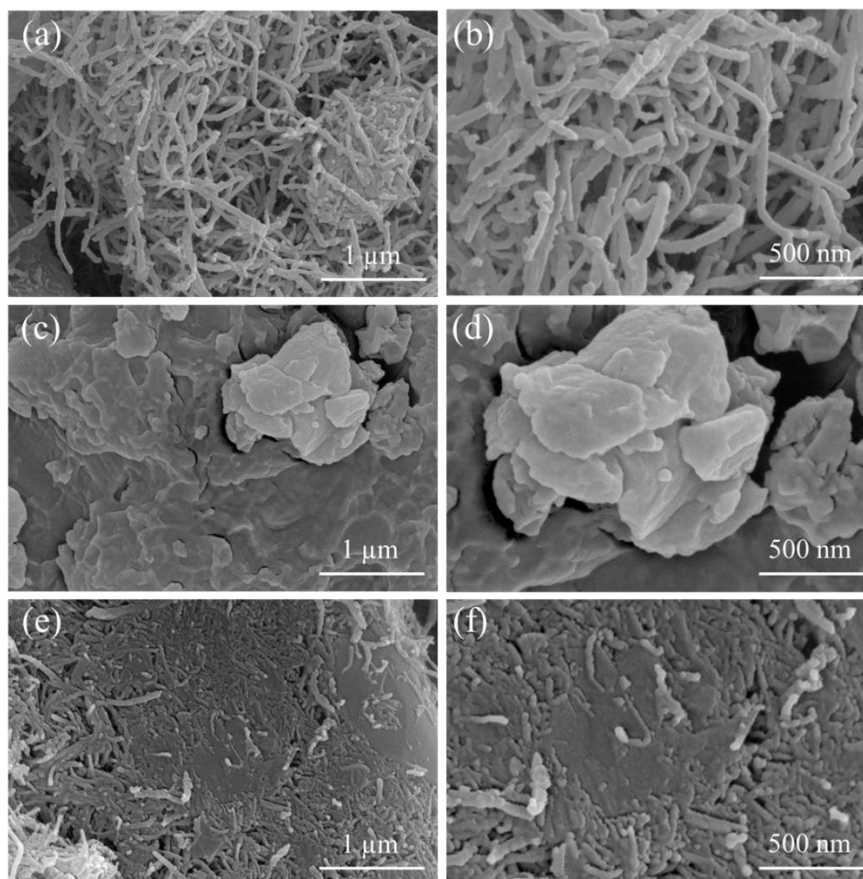


**Figure 1.** XRD spectra of (a) GR-MWCNTs-COOH, (b)  $\beta$ -CD and (c)  $\beta$ -CD/GR-MWCNTs-COOH.

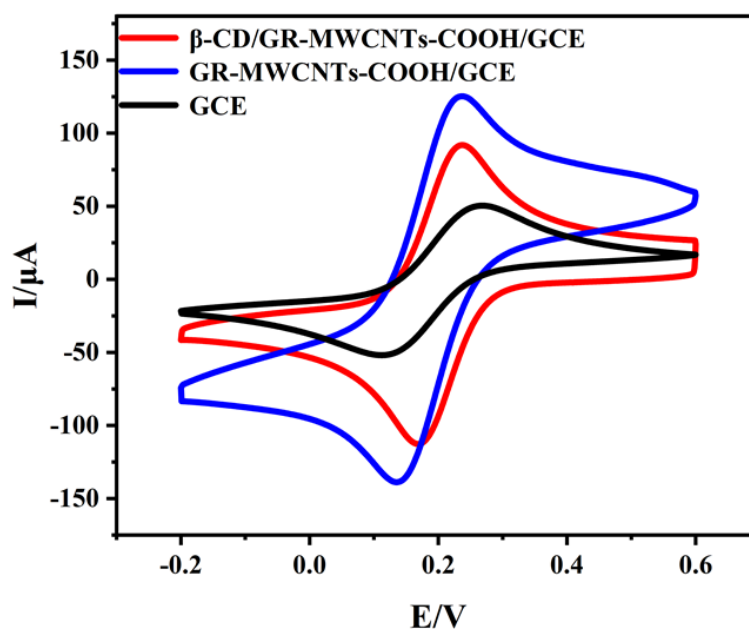
### 3. RESULTS AND DISCUSSION

The XRD patterns of GR-MWCNTs-COOH,  $\beta$ -CD and  $\beta$ -CD/GR-MWCNTs-COOH samples were shown in **Fig. 1**. It can be observed from **Fig. 1(a)** that there is an obvious characteristic diffraction peak in the XRD pattern of GR-MWCNTs-COOH. The sharp and narrow diffraction peak suggests the high graphitization degree, which means the excellent electrical conductivity [22]. There were no diffraction peaks of other impurities in the XRD pattern of GR-MWCNTs-COOH, suggesting the high purity. As shown in **Fig. 1(b)**, the XRD pattern of  $\beta$ -CD is completely different from that of GR-MWCNTs-COOH. For the  $\beta$ -CD/GR-MWCNTs-COOH composite, the corresponding XRD pattern contains several characteristic diffraction peaks of  $\beta$ -CD and GR-MWCNTs-COOH, which confirm the successful preparation of the  $\beta$ -CD/GR-MWCNTs-COOH nanocomposite.

The surface morphology of modification material has an important impact on the electrochemical performance of electrochemical sensor. **Fig. 2** shows the SEM images of GR-MWCNTs-COOH,  $\beta$ -CD, and  $\beta$ -CD/GR-MWCNTs-COOH samples. As shown in **Fig. 2(a, b)**, GR-MWCNTs-COOH presents one-dimensional nanostructure. The intertwined carbon network structure can be clearly observed in the SEM images with different magnifications. It can be found from **Fig. 2(c, d)** that some agglomerated particles appear in the SEM images of  $\beta$ -CD. **Fig. 2(e, f)** shows the SEM images of the  $\beta$ -CD/GR-MWCNTs-COOH nanocomposite at different magnifications. The obtained  $\beta$ -CD/GR-MWCNTs-COOH nanocomposite presents different surface morphology compared to the  $\beta$ -CD and GR-MWCNTs-COOH.

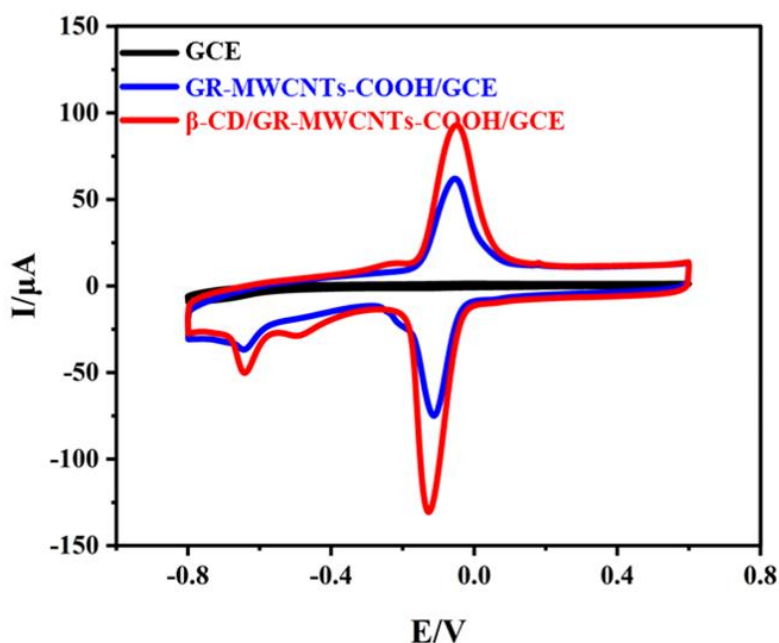


**Figure 2.** SEM images of (a, b) GR-MWCNTs-COOH, (c, d) β-CD, and (e, f) β-CD/GR-MWCNTs-COOH.



**Figure 3.** CV curves of the bare GCE, GR-MWCNTs-COOH/GCE, and β-CD/GR-MWCNTs-COOH/GCE at 100 mV s<sup>-1</sup> in 5 mM K<sub>3</sub>[Fe(CN)<sub>6</sub>]/K<sub>4</sub>[Fe(CN)<sub>6</sub>] solution containing 0.1m KCl.

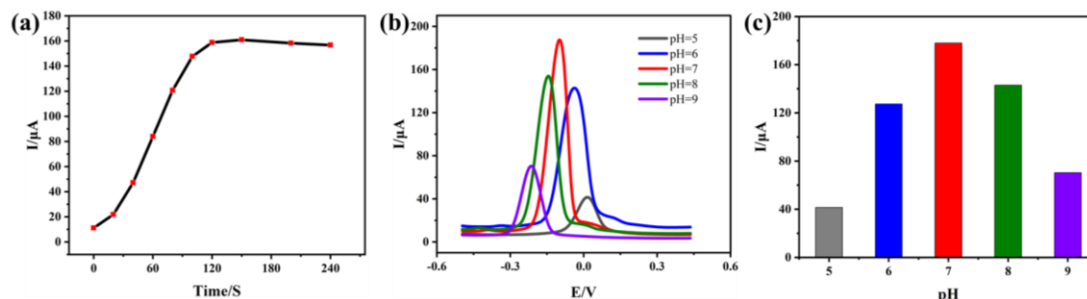
To investigate the electrochemical behavior of the  $\beta$ -CD/GR-MWCNTs-COOH/GCE sensor, the cyclic voltammetry (CV) measurement was performed, as shown in **Fig. 3**. It can be seen that the CV curve of the bare GCE sensor has a relatively weak reversible redox peak. After introducing GR-MWCNTs-COOH, the fabricated GR-MWCNTs-COOH/GCE sensor can present high reversible redox peak, which is closely related to the good electrical conductivity and large surface area of GR-MWCNTs-COOH [15, 17]. For the  $\beta$ -CD/GR-MWCNTs-COOH/GCE sensor, the corresponding peak current response is slightly smaller than that of the GR-MWCNTs-COOH/GCE sensor, which is attributed to the poor electrical conductivity of  $\beta$ -CD [23, 24].



**Figure 4.** CV curves of 50  $\mu$ M MP at the bare GCE, GR-MWCNTs-COOH/GCE, and  $\beta$ -CD/GR-MWCNTs-COOH/GCE sensors in 0.1 M PBS.

To investigate the electrochemical behavior of MP, the CV measurement of 50  $\mu$ M MP at the bare GCE, GR-MWCNTs-COOH/GCE, and  $\beta$ -CD/GR-MWCNTs-COOH/GCE sensors was performed in 0.1 M PBS solution (pH=7, Scanning rate: 100mV s<sup>-1</sup>), as shown in **Fig. 4**. No obvious reversible redox peak can be observed in the CV curve of the unmodified GCE sensor, suggesting the poor determination performance of MP. by contrast, the peak current response of GR-MWCNTs-COOH/GCE sensor is significantly increased due to the good electrical conductivity and large surface area of GR-MWCNTs-COOH. For the  $\beta$ -CD/GR-MWCNTs-COOH/GCE sensor, there is an irreversible reduction peak in the CV curve of 50  $\mu$ M MP, which corresponds to the fact that the nitro group is irreversibly reduced to hydroxylamine group [25, 26]. Moreover, a pair of reversible redox peaks can be clearly seen in the CV curve, which has much to do with the reversible reaction between hydroxylamine group and nitro group [27-29]. It is important to note that the  $\beta$ -CD/GR-MWCNTs-COOH/GCE sensor presents the highest peak current response. This result mainly benefits from the synergistic effect of  $\beta$ -CD and

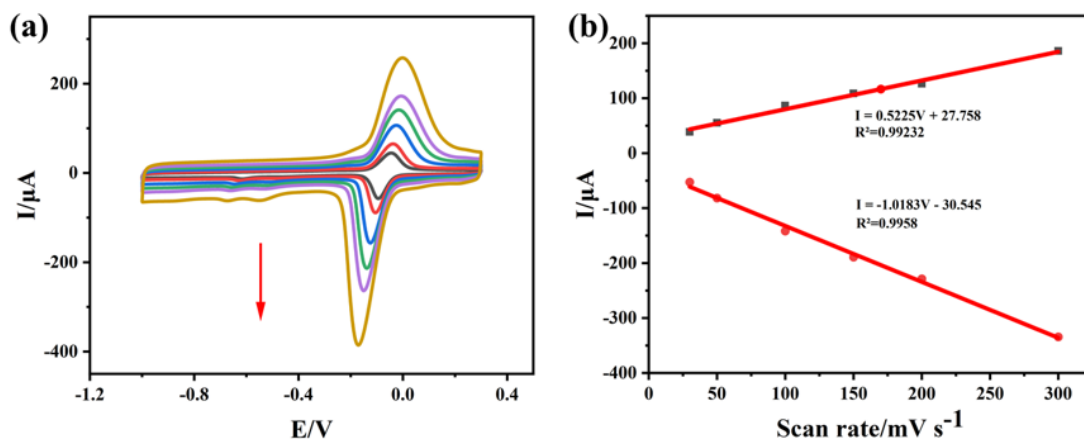
GR-MWCNTs-COOH. GR-MWCNTs-COOH has high electrical conductivity, large specific surface area, and good hydrophilicity [15, 17, 24].  $\beta$ -CD can effectively promote the uniform dispersion of GR-MWCNTs-COOH and possess excellent molecular recognition and selection ability for organic molecules [23, 24]. The combination of  $\beta$ -CD and GR-MWCNTs-COOH significantly enhances the MP determination performance at the  $\beta$ -CD/GR-MWCNTs-COOH/GCE sensor.



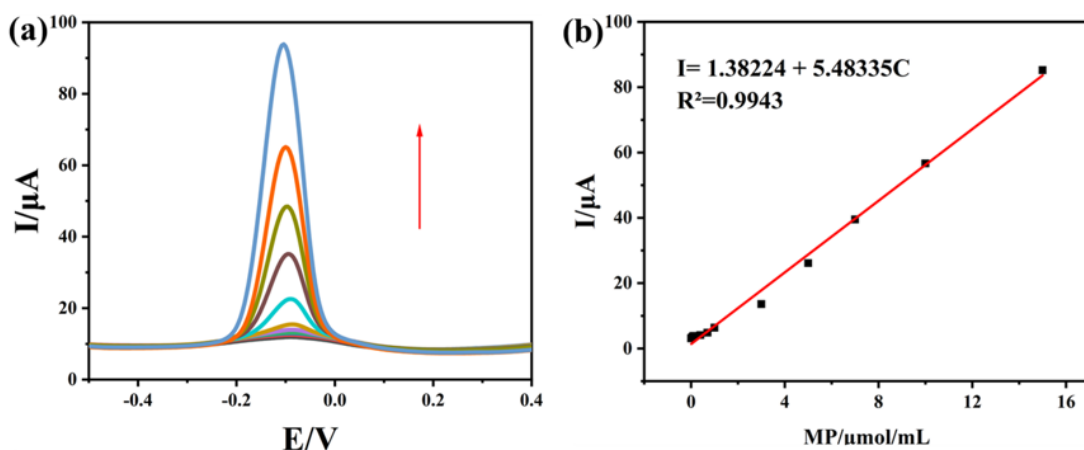
**Figure 5.** (a) Influence of enrichment time on oxidation peak current, (b) effect of pH value on the DPV curve of MP at the  $\beta$ -CD/GR-MWCNTs-COOH/GCE sensor, and (c) effect of pH on oxidation peak current.

To enhance the determination performance of MP, the influence of enrichment time on the current response was studied at the  $\beta$ -CD/GR-MWCNTs-COOH/GCE sensor, as shown in **Fig. 5(a)**. The peak current increased gradually with the increasing of enrichment time. When the enrichment time reaches up to 120 s, the corresponding peak current response did not show no obvious change. In order to improve the detection efficiency, 120 s is chosen as the optimal enrichment time for the determination of MP at the  $\beta$ -CD/GR-MWCNTs-COOH/GCE sensor.

The determination performance of MP is also affected by the pH value of PBS solution. To confirm the effect of pH value, the DPV curve of MP was investigated at the  $\beta$ -CD/GR-MWCNTs-COOH/GCE sensor, and the pH value range is from 5.0 to 9.0. **Fig. 5(b)** shows the effect of pH value on the DPV curve of MP at the  $\beta$ -CD/GR-MWCNTs-COOH/GCE sensor. It can be found from **Fig. 5(c)** that the peak current response of MP increases first and then decreases with the increasing of pH value. When the pH value is 7.0, the corresponding peak current response reaches up to the maximum value. In order to achieve the optimal determination of MP, the pH value of 7.0 is selected for the subsequent determination of MP.



**Figure 6.** (a) Influence of scanning rate on the CV curve of 50  $\mu\text{M}$  at the  $\beta\text{-CD/GR-MWCNTs-COOH/GCE}$  sensor and (b) linear relationship between peak current value and scanning rate.

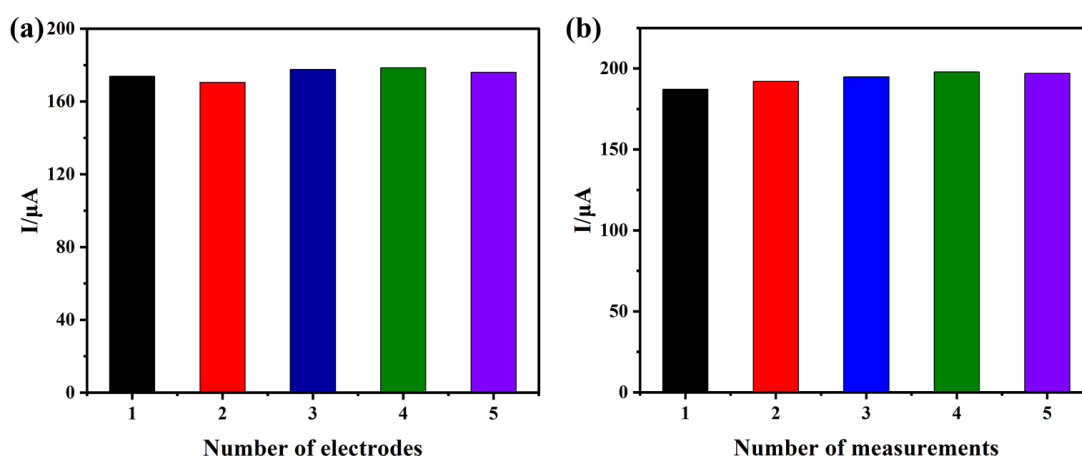


**Figure 7.** (a) Effect of MP concentration on the DPV curve at the  $\beta\text{-CD/GR-MWCNTs-COOH/GCE}$  sensor and (b) change relationship of anodic peak current with MP concentration (Concentration range: 0.01, 0.05, 0.1, 0.4, 0.7, 1, 3, 5, 7, 10, 15  $\mu\text{M}$ ).

**Fig. 6** shows the effect of scanning rate on the CV curve of 50  $\mu\text{M}$  at the  $\beta\text{-CD/GR-MWCNTs-COOH/GCE}$  sensor, and the corresponding scanning rates are 30, 50, 100, 150, 200, and 300  $\text{mV/s}$ , respectively. It can be obviously observed from **Fig. 6(a)** that the scanning rate produces an obvious impact on the CV curve of 50  $\mu\text{M}$ . As shown in **Fig. 6(b)**, the current response of oxidation peak and reversible reduction peak gradually increased with the increasing of scanning rate, and the peak-to-peak potential difference also gradually increased. Especially, the peak current value has a linear relationship with the scanning rate. The corresponding regression equations are described as  $I_{\text{O}} (\mu\text{A}) = 0.5225V + 27.758$  ( $R^2 = 0.99232$ ) and  $I_{\text{R}} (\mu\text{A}) = -30.545V - 1.0183$  ( $R^2 = 0.9958$ ). The above analysis result suggests that the electrochemical reaction of MP at the  $\beta\text{-CD/GR-MWCNTs-COOH/GCE}$  sensor belongs to the surface-controlled electrochemical process.

**Table 1** Comparison of different MP electrochemical sensors.

Electrode	Detection limit ( $\mu\text{M}$ )	Linear range ( $\mu\text{M}$ )	Reference
CNT/CPE	0.27	1.00-6.25	[30]
Nano-GO-SiO <sub>2</sub> -GCE	2.09	6.25-1000	[31]
PEI-rGO/GCE	0.41	0.59-59	[32]
ZrO <sub>2</sub> -ChCl-AuNPs/CPE	0.025	0.22-55	[33]
CS-Fe <sub>2</sub> O <sub>3</sub> -ERGO/GCE	0.15	1-100	[34]
$\beta$ -CD/GR-MWCNTs-COOH/GCE	0.027	0.01-15	This work

**Figure 8.** (a) Reproducibility and (b) repeatability of the  $\beta$ -CD/GR-MWCNTs-COOH/GCE sensor.

**Fig. 7(a)** shows the effect of MP concentration on the DPV curve at the  $\beta$ -CD/GR-MWCNTs-COOH/GCE sensor, and the corresponding MP concentration ranges are 0.01, 0.05, 0.1, 0.4, 0.7, 1, 3, 5, 7, 10, and 15  $\mu\text{M}$ . It can be observed from **Fig. 7(a)** that the oxidation peak current shows an obvious upward trend with the increase of MP concentration. **Fig. 7(a)** shows the change relationship of anodic peak current with MP concentration. The corresponding regression equation is described as  $I (\mu\text{A}) = 5.48335C + 1.38224$  ( $R^2 = 0.9943$ ). Based on the calculation result, the detection of limit can reach up to 0.027  $\mu\text{M}$ . **Table 1** lists the comparison of MP determination performance at the  $\beta$ -CD/GR-MWCNTs-COOH/GCE sensor and other reported sensors. It can be found that the fabricated  $\beta$ -CD/GR-MWCNTs-COOH/GCE sensor shows better MP determination performance compared to the reported sensors. This result mainly benefits from the synergistic effect of  $\beta$ -CD and GR-MWCNTs-COOH. GR-MWCNTs-COOH has high electrical conductivity, large specific surface area, and good hydrophilicity [15, 17, 24].  $\beta$ -CD can effectively promote the uniform dispersion of GR-MWCNTs-COOH and possess excellent molecular recognition and selection ability for organic molecules [23, 24]. The combination of  $\beta$ -CD and GR-MWCNTs-COOH significantly enhances the MP determination performance.

The reproducibility and repeatability are very important for the practical application of electrochemical sensor. The reproducibility measurement was performed based on five different  $\beta$ -CD/GR-MWCNTs-COOH/GCE sensors. **Fig. 8(a)** shows the peak current value of differential pulse voltammetry (DPV) curves of 50  $\mu\text{M}$  MP at the  $\beta$ -CD/GR-MWCNTs-COOH/GCE sensor. The peak

current responses of these sensors do not show obvious change, suggesting the good reproducibility. **Fig. 8(b)** shows the repeatability of the  $\beta$ -CD/GR-MWCNTs-COOH/GCE sensor. The reproducibility measurement was performed based on five repeatable determination measurement of 50  $\mu$ M MP at one  $\beta$ -CD/GR-MWCNTs-COOH/GCE sensor. The good consistency can be observed without obvious change, which suggests the good repeatability.

To confirm the practicability of the  $\beta$ -CD/GR-MWCNTs-COOH/GCE sensor, two real samples (tap water and lake water) were first filtered by using a standard 0.22  $\mu$ m filter and then spiked with MP standard solutions. All samples were measured for three times. The recovery of MP in each water sample is the average value of three measured concentration. **Table 2** lists the analytical result of MP in real samples using the proposed sensor. It can be found that the  $\beta$ -CD/GR-MWCNTs-COOH/GCE sensor presents satisfactory recoveries of 95.6%-100.1% and relative standard deviation (RSD) values of 2.03-4.09, which suggest the good practicability of the proposed sensor for the MP determination in real samples.

**Table 2.** Analytical results of MP in real samples using the  $\beta$ -CD/GR-MWCNTs-COOH/GCE sensor.

Sample	MP added ( $\mu$ M)	MP found ( $\mu$ M)	Recovery (%)	RSD (%)
Tap water	5.00	4.98	99.6	4.09
	10.00	9.75	97.5	3.18
Lake water	5.00	4.78	95.6	4.04
	10.00	10.01	100.1	2.03

#### 4. CONCLUSION

This work developed a novel  $\beta$ -CD/GR-MWCNTs-COOH/GCE sensor for the sensitive determination of MP based on the graphitized and carboxylated multi-walled carbon nanotubes@ $\beta$ -cyclodextrin nanocomposite modified GCE. Compared with the bare GCE sensor, the fabricated  $\beta$ -CD/GR-MWCNTs-COOH/GCE sensor could showed good MP determination performance with low detection of limit of 0.027  $\mu$ M in linear MP concentration range of 0.01-15  $\mu$ M. Such good determination performance had much to do with the synergistic effect between GR-MWCNTs-COOH and  $\beta$ -CD. This work could provide important reference value for the design of high-performance MP electrochemical sensor.

#### ACKNOWLEDGMENTS

This work was financially supported by the Research Project of Science and Technology of Henan Province (No. 202102210026), Basic Research of Henan Institute of Science and Technology (No. 203010617010), and University Students' Innovation and Pioneering Project of Henan Province (No. S202110467003).

#### References

1. Chansi, P.R. R, I. Mukherjee, T. Basu and L.M. Bharadwaj, *Nanoscale*, 12 (2020) 21719.

2. X. Gao, Y. Gao, C. Bian, H. Ma and H. Liu, *Electrochim. Acta*, 310 (2019) 78.
3. S. Nagabooshanam, A.T. John, S. Wadhwa, A. Mathur, S. Krishnamurthy and L.M. Bharadwaj, *Food Chem.*, 323 (2020) 126784.
4. K.P. Gannavarapu, V. Ganesh, M. Thakkar, S. Mitra and R.B. Dandamudi, *Sensor. Actuat. B Chem.*, 288 (2019) 611.
5. J. Yao, Z. Liu, M. Jin, Y. Zou, J. Chen, P. Xie, X. Wang, E.M. Akinoglu, G. Zhou and L. Shui, *Sensor. Actuat. B Chem.*, 321 (2020) 128517.
6. H. Karimi-Maleh, F. Karimi, M. Alizadeh and A.L. Sanati, *Chem. Rec.*, 20 (2020) 682.
7. H.L. Tcheumi, V.N. Tassontio, I.K. Tonle and E. Ngameni, *Appl. Clay Sci.*, 173 (2019) 97.
8. P. Qi, Z. Xu, T. Zhang, T. Fei and R. Wang, *J. Colloid Interface Sci.*, 560 (2020) 284.
9. C. Wang, J. Du, H. Wang, C.e. Zou, F. Jiang, P. Yang and Y. Du, *Sensor. Actuat. B Chem.*, 204 (2014) 302.
10. F. Li, R. Liu, V. Dubovyk, Q. Ran, B. Li, Y. Chang, H. Wang, H. Zhao and S. Komarneni, *Food Chem.*, 366 (2022) 130563.
11. C.O. Michelle, F.R. Caetano, M.A.P. Papi, E.Y. Watanabe, L.H. Marcolino-Júnior and M.F. Bergamini, *J. Anal. Chem.*, 75 (2020) 119.
12. K.d.S. Caetano, D.S. da Rosa, T.M. Pizzolato, P.A.M. dos Santos, R. Hinrichs, E.V. Benvenuti, S.L.P. Dias, L.T. Arenas and T.M.H. Costa, *Micropor. Mesopor. Mater.*, 309 (2020) 110583.
13. B. Huang, W.-D. Zhang, C.-H. Chen and Y.-X. Yu, *Microchim. Acta*, 171 (2010) 57.
14. S. Zhang, Y. Shao, G. Yin and Y. Lin, *Appl. Catal. B Environmen.*, 102 (2011) 372.
15. Y. Xue, S. Zheng, Z. Sun, Y. Zhang and W. Jin, *Chemosphere*, 183 (2017) 156.
16. C. Singh, S. Srivastava, M.A. Ali, T.K. Gupta, G. Sumana, A. Srivastava, R.B. Mathur and B.D. Malhotra, *Senso. Actuat. B Chem.*, 185 (2013) 258.
17. J. Li, D. Kuang, Y. Feng, F. Zhang and M. Liu, *Microchim. Acta*, 172 (2010) 379.
18. M. Ni, J. Chen, C. Wang, Y. Wang, L. Huang, W. Xiong, P. Zhao, Y. Xie and J. Fei, *Microchem. J.*, 178 (2022) 107410.
19. R. Liu, B. Li, F. Li, V. Dubovyk, Y. Chang, D. Li, K. Ding, Q. Ran, G. Wang and H. Zhao, *Food Chem.*, 384 (2022) 132573.
20. P. Balasubramanian, M. Annalakshmi, S.M. Chen, T. Sathesh and T.S.T. Balamurugan, *Ultrason. Sonochem.*, 52 (2019) 391.
21. R. Liu, Y. Wang, D. Li, L. Dong, B. Li, B. Liu, H. Ma, F. Li, X. Yin, X. Chen, *Int. J. Electrochem. Sci.*, 14 (2019) 9785.
22. H. Zhao, Q. Ran, Y. Li, B. Li, B. Liu, H. Ma, M. Zhang and S. Komarneni, *J. Mater. Res. Technol.*, 9 (2020) 9422.
23. W. Zhang, C. Liu, X. Zou, H. Zhang and Y. Xu, *Food Anal. Method.*, 12 (2019) 2326.
24. R. Liu, Y. Wang, B. Li, B. Liu, H. Ma, D. Li, L. Dong, F. Li, X. Chen and X. Yin, *Materials*, 12 (2019) 3637
25. H. Zhao, H. Ma, X. Li, B. Liu, R. Liu and S. Komarneni, *Appl. Clay Sci.*, 200 (2021) 105907.
26. H. Zhao, B. Liu, Y. Li, B. Li, H. Ma and S. Komarneni, *Ceram. Int.*, 46 (2020) 19713.
27. T. Tao, Y. Zhou, C. He, H. He, M. Ma, Z. Cai, N. Gao, K. Wang, R. Zhu, G. Chang, Z. Liu and Y. He, *Electrochim. Acta*, 357 (2020) 136836.
28. M. Stoytcheva, R. Zlatev, Z. Velkova, V. Gochev, G. Montero, B. Valdez and M. Curiel, *Electroanal.*, 32 (2020) 1.
29. R. Shanmugam, S. Manavalan, S.-M. Chen, M. Keerthi and L.-H. Lin, *ACS Sustain. Chem. Eng.*, 8 (2020) 11194.
30. S.M. Ghoreishi, M. Behpour, M. Khayatkashani and M.H. Motaghedifard, *Analytical Methods*, 3 (2011) 636.
31. C.O. Chikere, N.H. Faisal, P.K.T. Lin and C. Fernandez, *J. Solid State Electr.*, 23 (2019) 1795.
32. J.H. Luo, B.L. Li, N.B. Li and H.Q. Luo, *Sensor. Actuat. B Chem.*, 186 (2013) 84.
33. S.A. Shahamirifard, M. Ghaedi, Z. Razmi and S. Hajati, *Biosens. Bioelectron.*, 114 (2018) 30.

34. F. Gao, D.L. Zheng, H. Tanaka, F.P. Zhan, X.N. Yuan, F. Gao and Q.X. Wang, *Mat. Sci. Eng. C Mater.*, 57 (2015) 279

© 2022 The Authors. Published by ESG ([www.electrochemsci.org](http://www.electrochemsci.org)). This article is an open access article distributed under the terms and conditions of the Creative Commons Attribution license (<http://creativecommons.org/licenses/by/4.0/>).